Supplementary Figure 1

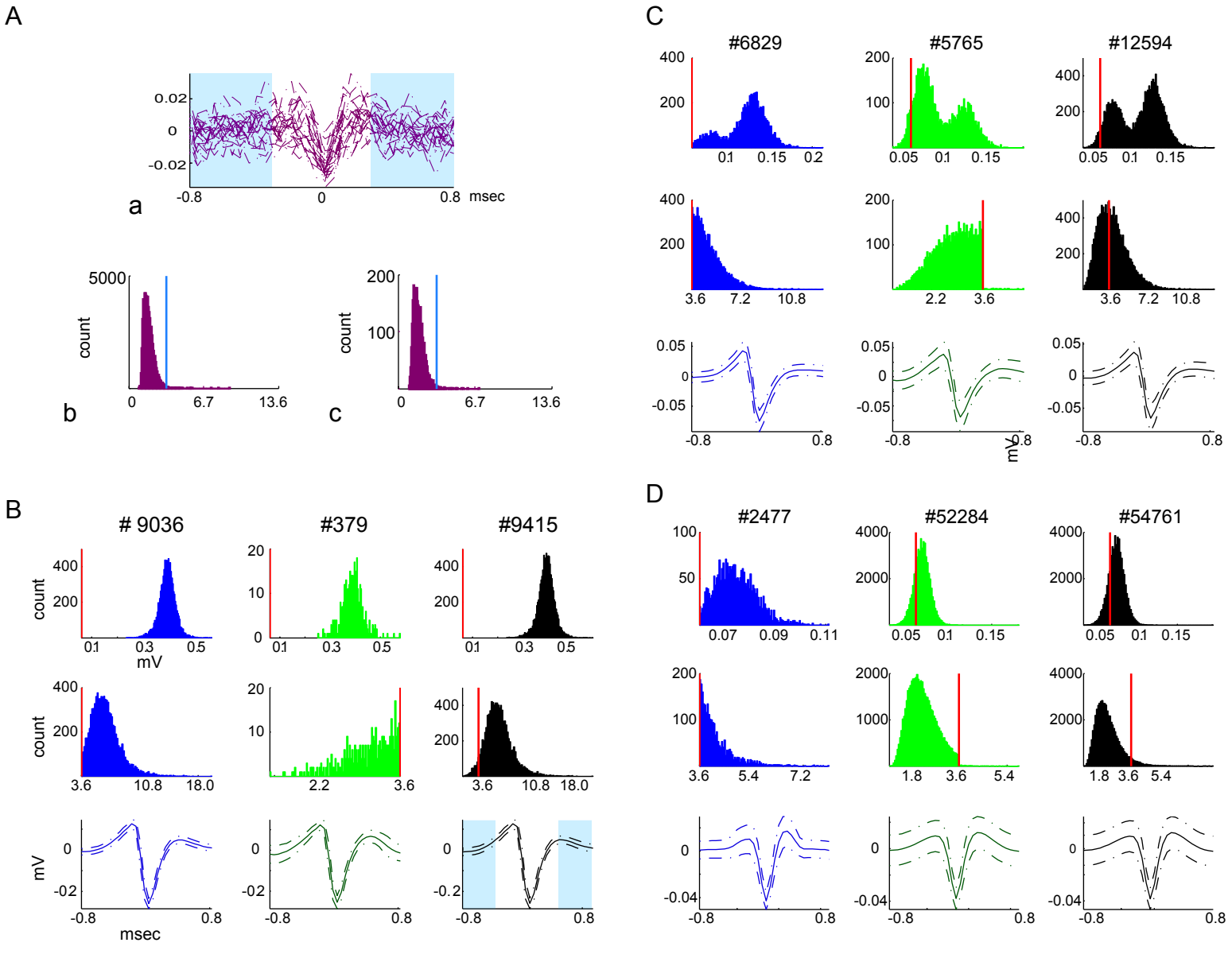

SI Figure 1. **Elimination of low-quality spikes**. A. Deriving signal-to-noise (SNR) threshold by extracting spike-frequency noise events from postmortem recordings. Aa. Overlaid traces of noise waveforms during TES. Ab. Noise-SNR distribution during stimulation free periods. Ac. Noise-SNR distribution during TES. An SNR-threshold of 3.60 was determined based on measurements across different electrodes. *Light blue shade*, period across which the standard deviation of the background noise was computed. *Cyan line*, SNR threshold. B, C, D. Spike-quality quantification for three units. B. Unit recorded in an anesthetized animal (stimulation as in *Fig 1.Ac*). C, D. Units recorded simultaneously during sleep (stimulation as in *Fig. 1Aa*). The number of events under each category is given on top of the 1st row. Top row, the distribution of peak-to-peak spike amplitudes. Middle row, SNR-distribution. Bottom row, mean waveform of spikes. *Red lines*, thresholds for the peak-to-peak spike-amplitude (60 µV, 1st row) and SNR (3.6, 2nd row). Right column (*black*), before noise-elimination. Middle column (*green*), eliminated events. Left (*blue*), after noise-elimination. Dashed lines, ±1 standard deviation. *Light blue shade*, periods across which the standard deviation of the background noise was computed. Spike-quality quantification and the noise-elimination were performed for the entire duration of recording session, prior to the analysis. Note that spike quality of the example units decreases from (*B*) to (*D*); and and progressively more spikes are discarded.

Supplementary Figure 2

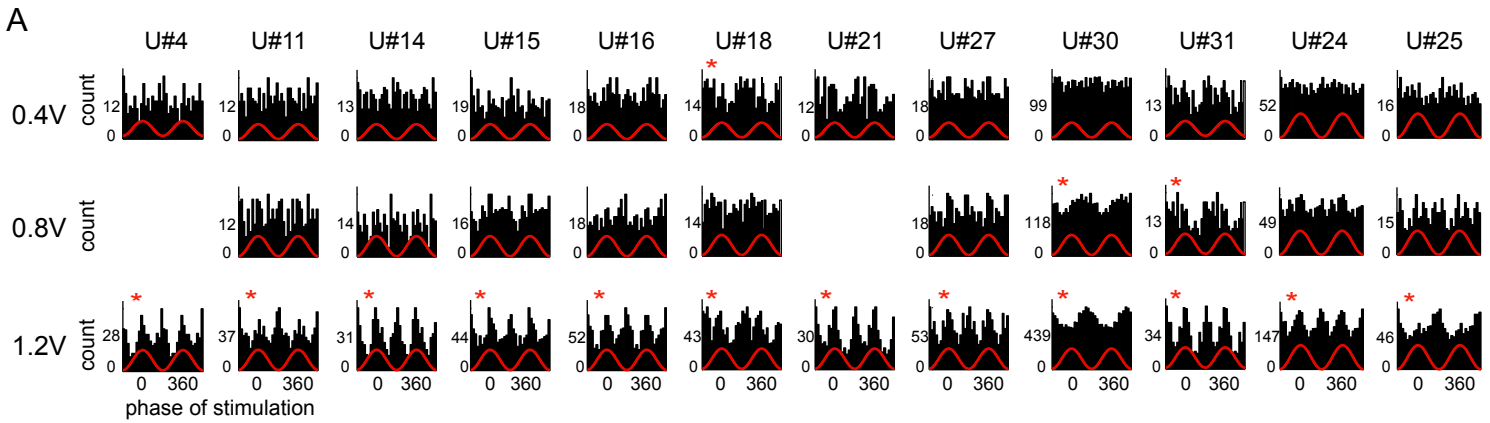

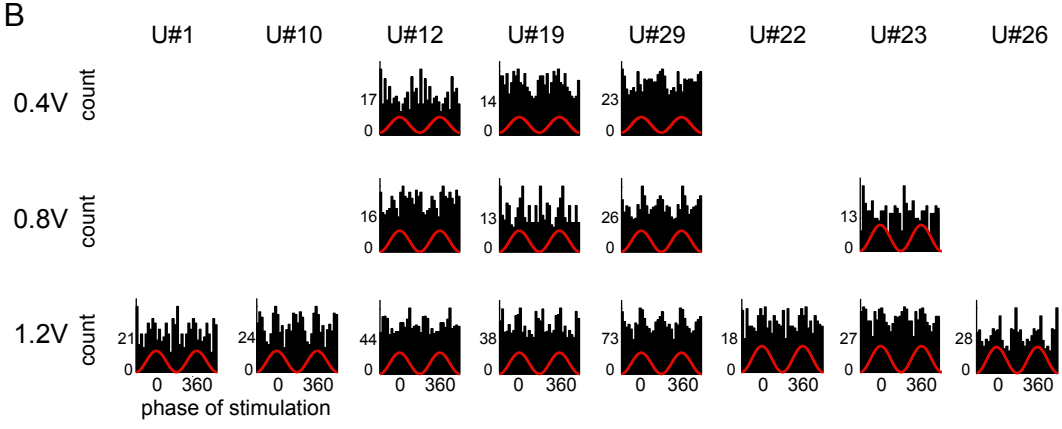

SI Figure 2. **TES intensity-dependent entrainment of unit firing**. Each histogram in A and B represents the activity of a single or multiple unit recorded simultaneously, under anesthesia (configuration; *Fig. 1Ac*) at 3 different stimulus intensities (weak 0.4 V, medium 0.8V, strong 1.2V; same experiment as in *Fig. 1D*). Empty spots refer to units excluded due to insufficient number of spikes (<250). A. Units, significantly modulated ($P<0.01$; Kuiper's test against uniformity) by at least one of the stimulation protocols. Red stars indicate the significant phase modulation ($P<0.01$, Kuiper's test). B. Non-modulated neurons. The fraction of TES-entrained neurons is overestimated because neurons firing at a low rate are not detected properly by clustering algorithms.

Supplementary Figure 3

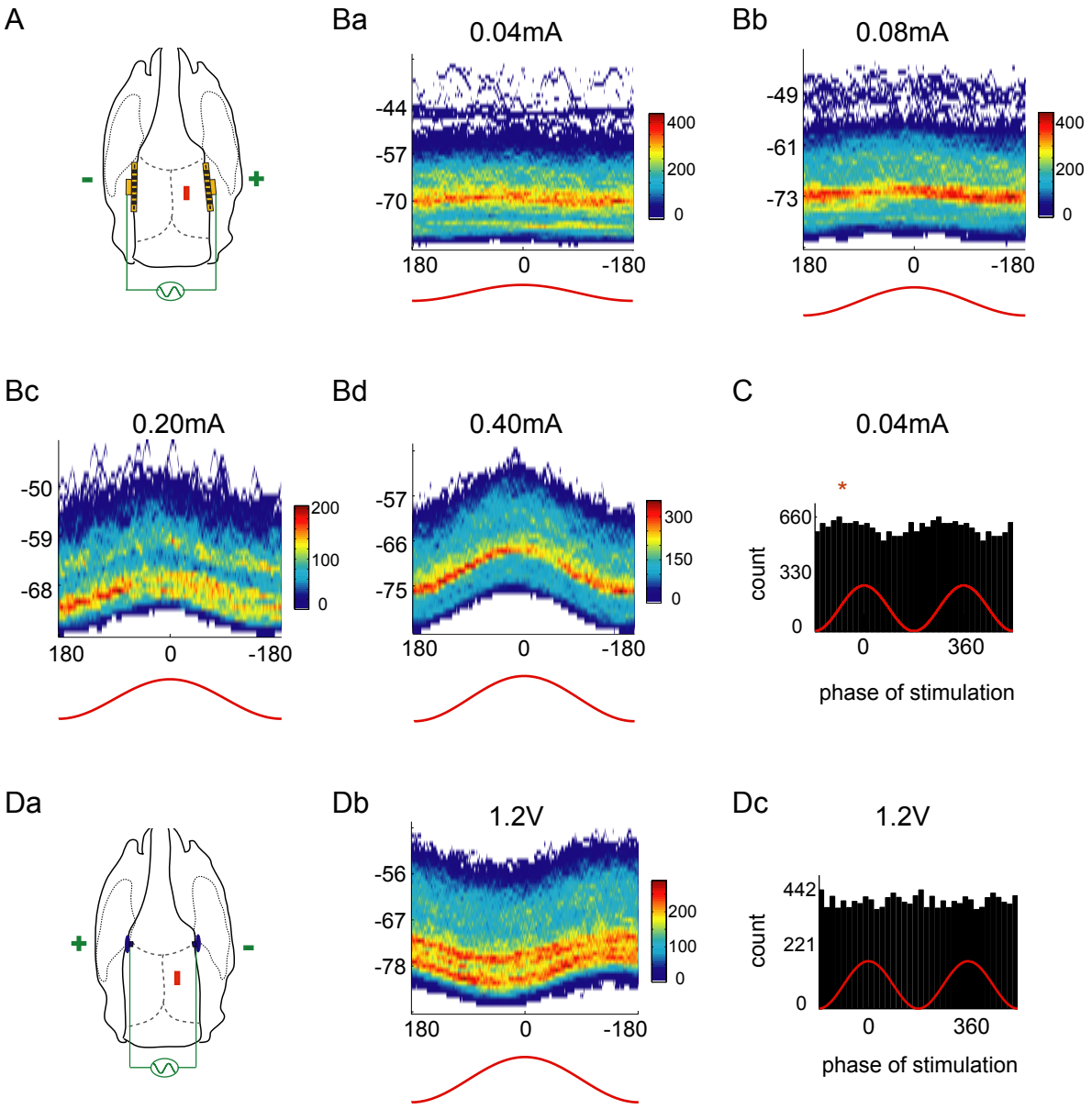

SI Figure 3. **Entrainment of subthreshold and suprathreshold neuronal activity by external fields**. A-B. Identical display as in *Fig.1D* for another intracellularly recorded layer V neuron in the somatosensory cortex (~980 μm). Aa. Stimulation configuration. Note that stimulation polarity is reversed compared to *D*, as well as *Fig 1D*. Red rectangle, recording site. Ba-d. Joint probability density of V_i with respect to the TES-phase for different intensities of 0.80 Hz stimulation (0.04 mA, 0.08 mA, 0.20 mA and 0.40 mA). In this experiment constant current stimulation was used. Red line, phase of stimulation. C. Histogram shows significant phase-modulation ($P<0.01$, Kuiper's test) of the discharge probability of action potentials as a function of the phase of the applied field (0.04 mA intensity). D. Same display for another intracellulary recorded neuron from the somatosensory area. Da. Stimulation configuration. Db. Joint probability density of V_i with respect to the TES-phase (1.25 Hz). Red line, phase of stimulation. Dc. Spike phase histogram showing the lack of phase-modulation of the discharge probability of the action potentials.

Supplementary Figure 4

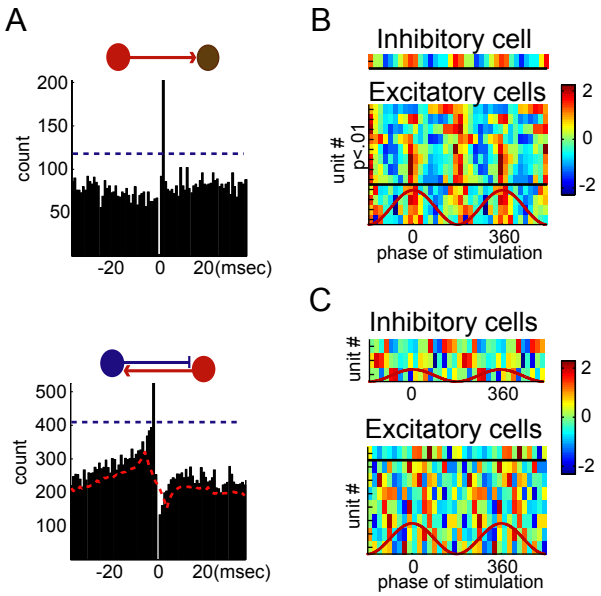

SI Figure 4. **Both excitatory and inhibitory neurons were affected by TES**. A. Example cross-correlograms between neuron pairs recorded in somatosensory cortex. Short-latency temporal interactions (< 5 msec) with other neurons can identify neurons as excitatory or inhibitory (Bartho et al., 2004; Isomura et al., 2006; Fujisawa et al., 2008; Sirota et al., 2008). Top, the red (reference) neuron excites the postsynaptic target neuron, as revealed by the short-latency large single bin. Bottom, bidirectional connectivity between a putative excitatory cell (red) and an inhibitory interneuron (reference blue). Note large peak before and transient suppression in the activity after the firing of the reference putative inhibitory neuron. Blue and red dashed lines, global maximum and point-wise minimum significance levels obtained by jittering (n=500) the cross-correlograms (Methods; Fujisawa et al., 2008). B and C. Subsets of the recorded neurons in two different experiments that were identified physiologically as putative excitatory or inhibitory cells (as in *A*). Significantly modulated units ($P<0.01$, Kuiper's Test) were grouped above the black line. B. Several excitatory neurons were entrained along with the interneuron. Stimulation configuration was as in *Fig 1Ac*. TES, 1.25 Hz, 1.2 V intensity. C. Only one excitatory neuron and none of the inhibitory neurons were affected. Stimulation configuration was in *Fig 1Aa*. TES, 1.25 Hz, 4.2 V intensity. These examples suggested that TES does not preferentially bias either population of neurons.

Supplementary Figure 5

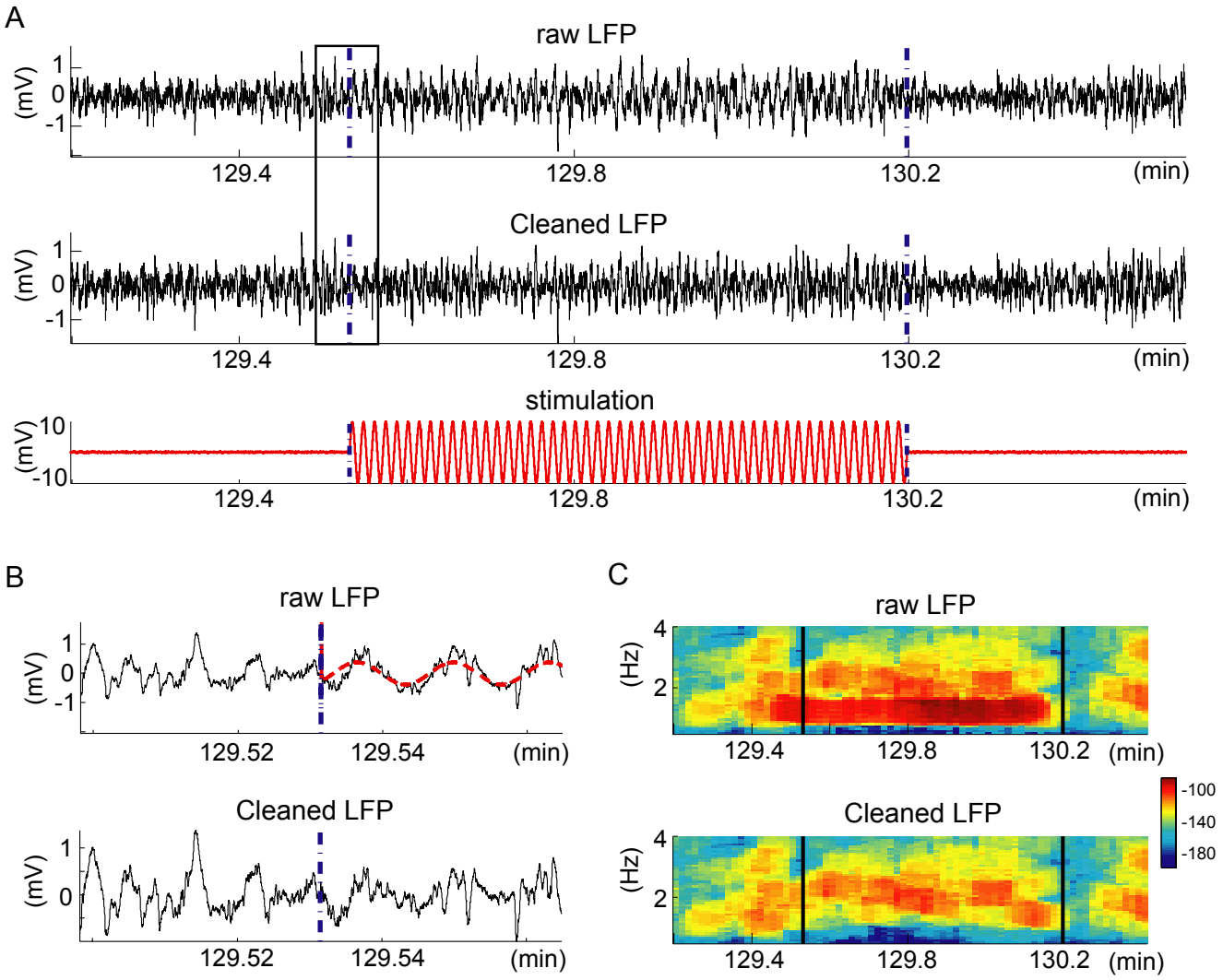

SI Figure 5. **Removal of additive TES field artifact from LFP.** A. LFP before, during and after TES (1 Hz to 5 kHz band-pass filtered). Note volume-conducted sinusoid pattern (added stimulation artifact). Below, LFP with the additive field artifact removed (Cleaned LFP). TES, 1.25 Hz, 1.6 V intensity. B. Zoomed-in segment from *A*. Top, raw LFP (black) with the volume-conducted signal (red), constructed by the procedure described in Methods. Bottom, after subtraction of the artifact from raw LFP. C. Time-resolved spectrograms of LFP before and after the removal of the stimulation artifact.

Supplementary References

Bartho P, Hirase H, Monconduit L, Zugaro M, Harris KD, Buzsaki G (2004) Characterization of neocortical principal cells and interneurons by network interactions and extracellular features. J Neurophysiol 92: 600-608.

Fujisawa S, Amarasingham A, Harrison MT, Buzsaki G (2008) Behavior-dependent short-term assembly dynamics in the medial prefrontal cortex. Nat Neurosci 11: 823-833.

Isomura Y, Sirota A, Ozen S, Montgomery S, Mizuseki K, Henze DA, Buzsaki G (2006) Integration and segregation of activity in entorhinal-hippocampal subregions by neocortical slow oscillations. Neuron 52: 871-882.

Sirota A, Montgomery S, Fujisawa S, Isomura Y, Zugaro M, Buzsaki G (2008) Entrainment of neocortical neurons and gamma oscillations by the hippocampal theta rhythm. Neuron 60: 683-697.